ChemComm

Accepted Manuscript

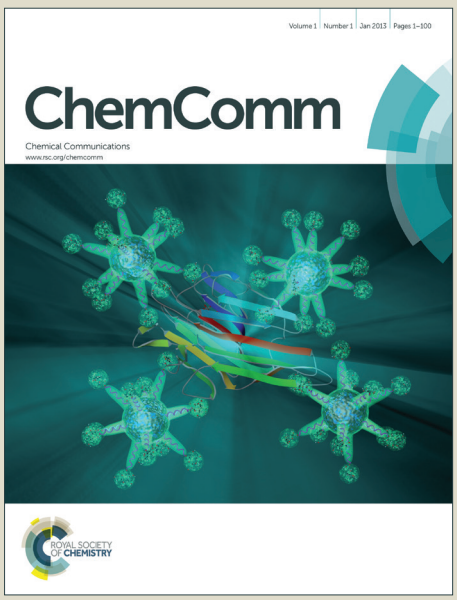

ROYAL SOCIETY OF CHEMISTRY

www.rsc.org/chemcomm

ChemComm

RSCPublishing

COMMUNICATION

Nitrogen-doped carbon dots decorated onto graphene: a novel all-carbon hybrid electrocatalyst for enhanced oxygen reduction reaction

Cite this: DOI: 10.1039/xoxxoooooox

Received ooth January 2012,
Accepted ooth January 2012

DOI: 10.1039/xoxxoooooox

www.rsc.org/

Chao Hu, Chang Yu, Mingyu Li, Xiuna Wang, Qiang Dong, Gang Wang, Jieshan Qiu*

An all-carbon hybrid, composed of coal-based nitrogen-doped carbon dots decorated onto graphene, was prepared via a hydrothermal treatment. The hybrid possesses a comparable electrocatalytic activity, better durability and methanol tolerance than those of the commercial Pt-based electrocatalysts for oxygen reduction reaction, indicative of a great potential in fuel cells.

The cathodic oxygen reduction reaction (ORR) is one of the most crucial factors for affecting the performance of a fuel cell. Currently, most efficient catalysts available for ORR are still Pt-based materials.[1] However, the high cost and limited availability of those materials have hampered their large-scale application. In this case, replacing precious and nondurable Pt catalysts with inexpensive and commercially available materials is one of key issues in the development of fuel cell technology. Recently, considerable efforts have been devoted to develop nonprecious-metal and metal-free catalysts as an alternative to Pt-based catalysts for ORR.[2] Inorganic metal oxides, hydroxides, sulfides, and metal-nitrogen doped into the graphene or carbon nanotubes as hybrid catalysts were demonstrated to improve the electrocatalytic activity for ORR in fuel cells.[3] Yet despite all that, metal-containing catalysts are still less preferable for ORR, because the acidic or basic media can make many metals leach from the electrode surfaces over time, causing the deactivation of the electrocatalysts. Certain heteroatom-doped carbon nanomaterials, such as carbon nanotubes,[2a, 4] graphene,[5] porous carbon,[6] were also suggested to act as effective metal-free ORR electrocatalysts. They not only exhibit excellent electrocatalytic activity, but also possess the advantages of low cost and environmental friendliness. Among the carbon material family, nitrogen-doped carbon dots (N-CDs) show a good electrocatalytic activity because of their distinctively physicochemical properties,[7] especially there are amounts of defects at the surface and edges which are considered as encouraging catalytic sites.[2b, 7b, 8] Nevertheless, the electron transfer can be restricted due to relatively low conductivity to some degree. Graphene is supposed to be an unique atom-thick two-dimensional structure, that is, an ideal support for catalyst attachment and electron transfer. It has been revealed that the graphene edge shows much faster electron transfer rate and stronger electrocatalytic activity than those of its basal plane.[9] Accordingly, combining the N-CDs and graphene into one electrode material and configuring multifunctional graphene-based electrocatalysts with abundant edges would be a feasible strategy for an enhanced catalytic activity towards ORR.

Herein, we developed an all-carbon-based hybrid composed of amounts of N-CDs onto graphene surface, and investigated their electrochemical performance as catalyst for ORR. This hybrid is abbreviated as N-CDs/G in the following sections. N-CDs decorate onto graphene surface and play the important role as catalytic sites, while graphene acts as a support to anchor and disperse N-CDs for avoiding large aggregates of CDs and benefit fast electron transfer. It is revealed that the N-CDs/G hybrid exhibits an excellent electrocatalytic activity, being comparable to that of commercial Pt-based catalyst. The stability and tolerance to crossover effect of the hybird are even better than those of the Pt-based catalyst, indicating a great potential as an ideal Pt alternative for ORR in fuel cells.

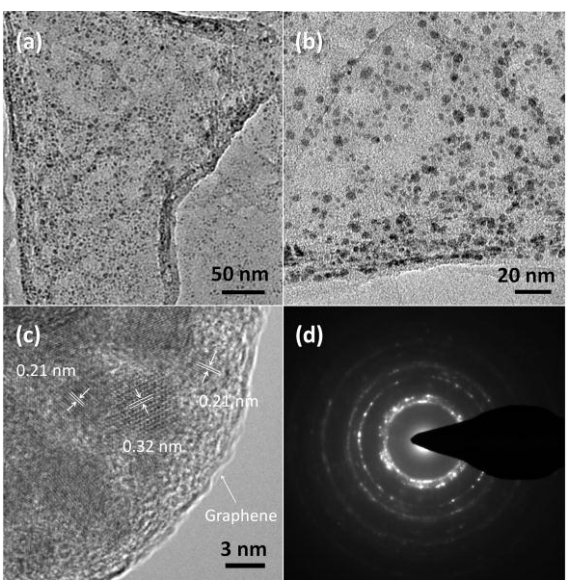

Fig. 1 (a) TEM image of the N-CDs/G hybrid. Scale bar, 50 nm. (b) Enlarged TEM image of the N-CDs/G hybrid. Scale bar, 20 nm. (c) High-resolution TEM image of the N-CDs/G hybrid. Scale bar, 3 nm. (d) SAED pattern of the N-CDs/G hybrid.

N-CDs were prepared by electrochemical etching of coal-based rod in an ammonia-containing electrolyte. Then, the N-CDs were combined with graphene oxide via a hydrothermal treatment to configure N-CDs/G hybrid (see ESI for more details). Transmission electron microscopy (TEM) images of the N-CDs/G hybrid are shown in Fig. 1, in which N-CDs are uniformly anchored onto the surface of graphene. Enlarged TEM image (Fig. 1b) reveals that the sizes of N-CDs are in a range of 2-6 nm. Fig. 1c shows the high-resolution TEM image of the N-CDs/G hybrid, in which the lattice spacing of 0.21 nm corresponds to the (100) crystal face of graphite. In addition, observation in Fig. 1c also confirms a 0.32 nm interlayer spacing for the few-layer N-CDs or graphitic crystallites. Selected area electron diffraction (SAED) of the N-CDs/G hybrid in Fig. 1d shows a ring-like diffraction pattern with dispersed bright spots. Such an amorphous structure is partially attributed to the existence of N-CDs with abundant edges and nitrogen doping defects. The oxygen-containing functional groups and defects on the graphene would benefit anchoring of N-CDs for avoiding large aggregates. The strong interaction between the N-CDs and graphene was further proved by the quenched fluorescence of the N-CDs after combination with graphene (Fig. S1).

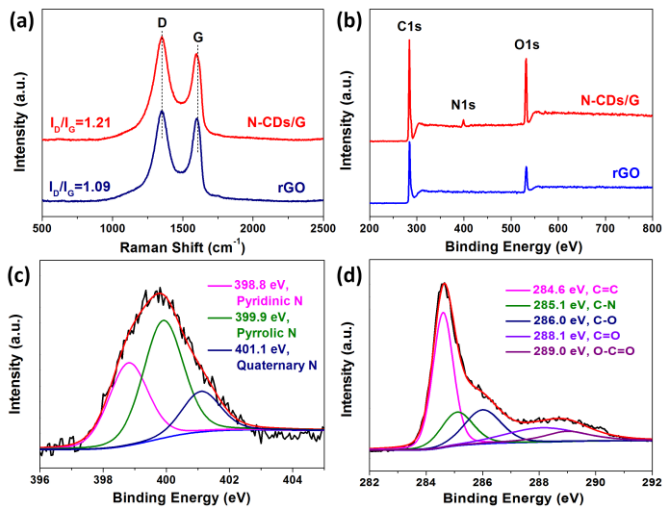

Fig. 2 (a, b) Raman spectra (a) and XPS spectra (b) of the N-CDs/G and the rGO. (c, d) High-resolution N 1s (c) and C 1s (d) spectra of the N-CDs/G hybrid.

Fig. 2a shows the Raman spectra of the N-CDs/G and the reduced graphene oxide (rGO) which originated from hydrothermal treatment of GO under the same conditions employed for the synthesis of N-CDs/G. Both spectra feature distinct peaks at ~1590 cm^{-1} and ~1350 cm^{-1} that correspond to the G and D bands, respectively. The ratio of the D and G band intensities (I_D/I_G) of the N-CDs/G hybrid is calculated to be 1.21, which is larger than that of the rGO. The increase of the I_D/I_G value after the involvement of N-CDs might be attributable to the presence of surface defects in the N-CDs structure. X-ray photoelectron spectroscopy (XPS) spectra of the N-CDs/G hybrid and the rGO are observed in Fig. 2b. It can be seen that both prepared rGO samples feature a prominent graphitic C1s peak at ~284 eV and an O1s peak at ~532 eV. The oxygen content is slightly increased after the involvement of the N-CDs. In addition to the C1s and O1s peaks, a new N1s peak at ~400 eV is also observed for the N-CDs/G hybrid, due to the incorporation of the N-doped CDs. The N/C atomic ratio is calculated to be 3.75%, close to that of the reported nitrogen-doped carbon nanomaterials used for ORR.[8a, 10] The high-resolution XPS N1s spectrum given in Fig. 2c reveals the presence of pyridinic, pyrrolic and quaternary nitrogen atoms within the N-CDs structure. In addition to the C-N bond, the high-resolution C1s spectrum of N-CDs/G further indicates the C-O, C=O, O-C=O configurations at 286.0 eV, 288.1 eV and 289.0 eV, respectively. A large portion of these oxygen-containing functional groups are suggested to locate at the edges of N-CDs in order to terminate dangling bonds of the edges.[11] As a result, the existence of the oxygen-containing groups with high polarity can make the N-CDs more hydrophilic in alkaline condition, leading to a stronger affinity to the electrolyte and dissolved oxygen.[9a]

The electrocatalytic activity of the N-CDs/G hybrid towards ORR was first examined by cyclic voltammetry in a 0.1 M KOH solution saturated with argon or oxygen. For comparison, commercial 20 wt.% platinum on carbon black (Pt/C) was also tested. All those electrocatalysts were separately loaded onto a glassy carbon (GC) electrode for measurement. As shown in Fig. 3a, featureless voltammetric currents within the potential range from –1.0 to +0.2 V are observed for the N-CDs/G in argon-saturated solution. In contrast, when the electrolyte solution is saturated with O_2, a well-defined cathodic peak centered at –0.25 V appears in the CV. This value is much higher than that of the bare GC electrode (–0.44 V, Supplementary Fig. S3) and comparable to the Pt/C catalyst as shown in Fig. 3b, suggesting a pronounced electrocatalytic activity of the N-CDs/G for ORR. As we know, the fuel molecules such as methanol and glucose in the anode sometimes permeate through the polymer membrane to the cathode and seriously affect the performance of the cathode catalysts. In this case, it is of great importance to consider and investigate the possible crossover effect for a new electrocatalyst. The electrocatalytic selectivities of the N-CDs/G and the Pt/C catalysts against the electrooxidation of methanol were also measured by cyclic voltammetry in an O_2-saturated 0.1 M KOH solution in the presence of methanol (10%, v/v). As can be seen in Fig. 3a, no obvious changes are observed for the N-CDs/G electrode upon addition of methanol into the O_2-saturated 0.1 M KOH solution, whereas a strong response for the commercial Pt/C catalyst is detected under the same conditions (Fig. 3b). That is to say, the N-CDs/G exhibits a high selectivity for ORR with a remarkably good ability to avoid crossover effect, being superior to the commercial Pt/C catalyst.

To further investigate the role of the N-CDs/G catalyst during ORR electrochemical process, we continued to compare its electrocatalytic performance with that of rGO, non-nitrogen doped CDs/G, and commercial Pt/C catalyst by linear sweep voltammetry in an O_2-saturated 0.1 M KOH solution. The same amount of each catalyst was loaded onto a GC rotating disk electrode (RDE). It is readily seen from Fig. 3c that the onset potential of the N-CDs/G electrode for ORR is much positive than that of the rGO as well as the CDs/G electrode, whereas relatively more negative than that of Pt/C electrode. The oxygen reduction current densities of the N-CDs/G electrode are also much larger than those of the rGO and the CDs/G electrode. These findings suggest the remarkable significance of the N-CDs in enhancing the electrocatalytic activity of the hybrid catalyst. N-CDs structure involves not only abundant edges and defect sites which are beneficial for the ORR catalytic activity, but also amounts of doped nitrogen atoms which can change the electronic structure of CDs and the chemisorption mode of O_2 and weaken the O-O bonding, further facilitating ORR at the N-CDs/G electrode.[2a, 12]

Fig. 3d shows the RDE voltammograms for ORR on the N-CDs/G electrode at various rotation speeds. As expected, the current density shows a typical increase with an increase of rotation speed due to the shortened diffusion layer. The kinetic parameters can be determined on the basis of the Koutechy-Levich (K-L) equations (ESI). As shown in Fig. 3e, the corresponding K-L plots at various electrode

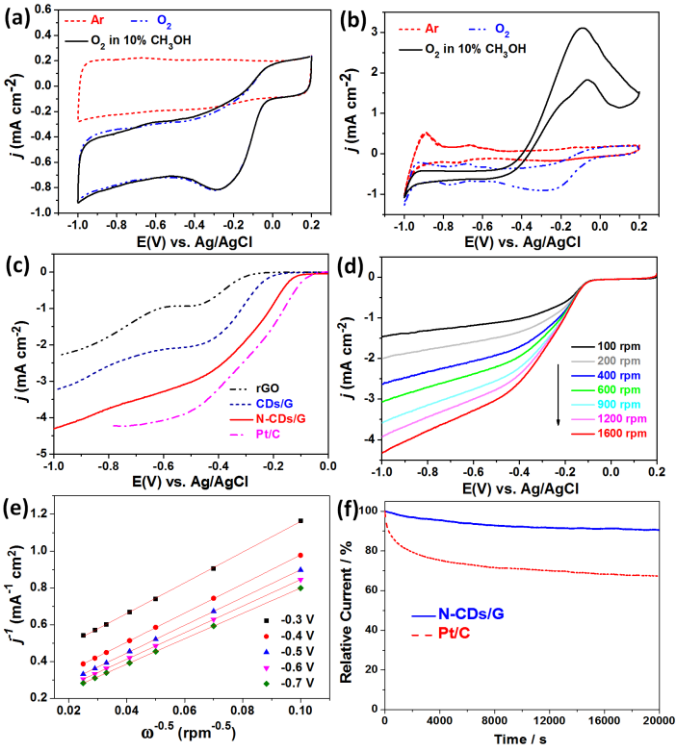

Fig. 3 (a, b) Typical cyclic voltammograms for ORR at N-CDs/G electrode (a) and Pt/C electrode (b) in a Ar- and O_2-saturated 0.1 M KOH solution, and an O_2-saturated 0.1 M solution of KOH upon addition of CH_3OH (10%, v/v). Scan rate: 50 mV s^{-1}. (c) RDE voltammograms of rGO electrode, CDs/G electrode, N-CDs/G electrode, and Pt/C electrode in an O_2-saturated 0.1 M KOH solution at a rotation rate of 1600 rpm. Scan rate: 10 mV s^{-1}. (d) RDE voltammograms of N-CDs/G electrode at different rotation rates. (e) K-L plots of j^{-1} versus $\omega^{-0.5}$ at the electrode potentials of –0.3, –0.4, –0.5, –0.6, and –0.7 V. Inset presents the calculated numbers of transferred electrons at these specified potentials. (f) Current-time (i-t) chronoamperometric responses for ORR at N-CDs/G and Pt/C electrodes at –0.25 V in an O_2-saturated 0.1 M KOH solution.

potentials exhibit a good linearity, indicating a first-order reaction kinetics with respect to the concentration of dissolved O_2. The dependence of the transferred electron number (n) on the potential in the case of the N-CDs/G electrode is shown as an inset in Fig. 3e. The n is estimated to be 3.6-4.0 at potentials ranging from –0.4 to –0.7 V (Fig. S4, ESI), suggesting a four-electron pathway for ORR on the N-CDs/G electrode. In contrast, the n is estimated to be 2.3-2.8 for the rGO, which explains that the ORR process catalyzed by the rGO is a two-electron process (Fig. S5, ESI). After doping with nitrogen-free CDs, the n for the CDs/G increases to 2.9-3.4 (Fig. S6, ESI), whereas still lower than that of N-CDs/G.

To further evaluate the stability of the N-CDs/G catalyst and the commercial Pt/C electrode, chronoamperometric responses were measured at a fixed potential of –0.25 V in a 0.1 M KOH solution saturated with O_2 at a rotation rate of 1000 rpm. As shown in Fig. 3f, the current density for the commercial Pt/C catalyst decreases rapidly with an approximately 32.9% current loss after 20000 s, whereas the N-CDs/G exhibites a relatively slow attenuation with a high current retention (90.6%), indicating that the stability of the N-CDs/G is much better than commercial Pt/C catalyst towards ORR in alkaline medium. The remarkable stability for the N-CDs/G is attributed to the excellent compatibility and strong interaction between the N-CDs and the graphene support during the reaction.

In summary, we have developed a hydrothermal approach to synthesize an all-carbon hybrid electrocatalyst, which is composed of graphene as a support and N-CDs as the catalytic sites. The material exhibits a competitive electrocatalytic activity, and high selectivity and better stability in comparison to commercial Pt-based catalyst in an alkaline medium. The electron transfer number for ORR at the N-CDs/G electrode is *ca.* 3.8, indicating that the dominant process is a favourable 4e- reduction pathway and thus showing high promise as a low-cost and efficient metal-free catalyst towards ORR. This type of hybrid will provide an opportunity to design and develop various metal-free, efficient ORR catalysts, which are essential for practical applications in fuel cells. Optimization and fabrication studies on N-CDs/G materials are underway.

This work was partly supported by the National Natural Science Foundation of China (Nos. 21336001, 51372028, U1203292).

Notes and references

Carbon Research Laboratory, Liaoning Key Lab for Energy Materials and Chemical Engineering, State Key Lab of Fine Chemicals, School of Chemical Engineering, Dalian University of Technology, Dalian, 116024, P. R. China, E-mail: jqiu@dlut.edu.cn

† Electronic Supplementary Information (ESI) available. See DOI: 10.1039/c000000x/

1. A. Morozan, B. Jousselme and S. Palacin, *Energy Environ. Sci.*, 2011, **4**, 1238-1254.
2. (a) K. Gong, F. Du, Z. Xia, M. Durstock and L. Dai, *Science*, 2009, **323**, 760-764; (b) Y. Li, W. Zhou, H. Wang, L. Xie, Y. Liang, F. Wei, J. C. Idrobo, S. J. Pennycook and H. Dai, *Nat. Nanotechnol.*, 2012, **7**, 394-400; (c) Y. Liang, Y. Li, H. Wang, J. Zhou, J. Wang, T. Regier and H. Dai, *Nat. Mater.*, 2011, **10**, 780-786; (d) P. Chen, T. Y. Xiao, Y. H. Qian, S. S. Li and S. H. Yu, *Adv. Mater.*, 2013, **25**, 3192-3196.
3. (a) Y. Liang, Y. Li, H. Wang and H. Dai, *J. Am. Chem. Soc.*, 2013, **135**, 2013-2036; (b) J. Duan, Y. Zheng, S. Chen, Y. Tang, M. Jaroniec and S. Qiao, *Chem. Commun.*, 2013, **49**, 7705-7707; (c) L. Wang, J. Yin, L. Zhao, C. Tian, P. Yu, J. Wang and H. Fu, *Chem. Commun.*, 2013, **49**, 3022-3024.
4. L. Yang, S. Jiang, Y. Zhao, L. Zhu, S. Chen, X. Wang, Q. Wu, J. Ma, Y. Ma and Z. Hu, *Angew. Chem. Int. Ed.*, 2011, **50**, 7132-7135.
5. (a) S. Yasuda, L. Yu, J. Kim and K. Murakoshi, *Chem. Commun.*, 2013, **49**, 9627-9629; (b) L. Qu, Y. Liu, J. B. Baek and L. Dai, *ACS Nano*, 2010, **4**, 1321-1326.
6. (a) R. Liu, D. Wu, X. Feng and K. Müllen, *Angew. Chem. Int. Ed.*, 2010, **49**, 2565-2569; (b) R. Silva, D. Voiry, M. Chhowalla and T. Asefa, *J. Am. Chem. Soc.*, 2013, **135**, 7823-7826.
7. (a) W. Li, Z. Zhang, B. Kong, S. Feng, J. Wang, L. Wang, J. Yang, F. Zhang, P. Wu and D. Zhao, *Angew. Chem. Int. Ed.*, 2013, **52**, 8151-8155; (b) C. Zhu, J. Zhai and S. Dong, *Chem. Commun.*, 2012, **48**, 9367-9369; (c) Y. Xu, M. Wu, Y. Liu, X.-Z. Feng, X.-B. Yin, X.-W. He and Y.-K. Zhang, *Chem. Eur. J.*, 2013, **19**, 2276-2283; (d) C. Hu, C. Yu, M. Li, X. Wang, J. Yang, Z. Zhao, A. Eychmüller, Y. P. Sun and J. Qiu, *Small*, 2014, **10**, 4926-4933.
8. (a) Y. Li, Y. Zhao, H. Cheng, Y. Hu, G. Shi, L. Dai and L. Qu, *J. Am. Chem. Soc.*, 2012, **134**, 15-18; (b) Q. Li, S. Zhang, L. Dai and L.-s. Li, *J. Am. Chem. Soc.*, 2012, **134**, 18932-18935.
9. (a) W. Yuan, Y. Zhou, Y. Li, C. Li, H. Peng, J. Zhang, Z. Liu, L. Dai and G. Shi, *Sci. Rep.*, 2013, **3**, 2248; (b) D. Deng, L. Yu, X. Pan, S. Wang, X. Chen, P. Hu, L. Sun and X. Bao, *Chem. Commun.*, 2011, **47**, 10016-10018.
10. D. Yu, Q. Zhang and L. Dai, *J. Am. Chem. Soc.*, 2010, **132**, 15127-15129.
11. D. Pan, J. Zhang, Z. Li and M. Wu, *Adv. Mater.*, 2010, **22**, 734-738.
12. M. Zhang and L. Dai, *Nano Energy*, 2012, **1**, 514-517.